Histone acetylation of glucose-induced thioredoxin-interacting protein gene expression in pancreatic islets

Bompada, Pradeep

2016-12

Bompada , P , Atac , D , Luan , C , Andersson , R , Omella , J D , Laakso , E O , Wright , J , Groop , L & De Marinis , Y 2016 , ' Histone acetylation of glucose-induced thioredoxin-interacting protein gene expression in pancreatic islets ' , International Journal of Biochemistry & Cell Biology , vol. 81 , pp. 82-91 . https://doi.org/10.1016/j.biocel.2016.10.022

http://hdl.handle.net/10138/231342
https://doi.org/10.1016/j.biocel.2016.10.022

publishedVersion

The International Journal of Biochemistry & Cell Biology 81 (2016) 82–91

Contents lists available at ScienceDirect

The International Journal of Biochemistry & Cell Biology

journal homepage: www.elsevier.com/locate/biocel

Histone acetylation of glucose-induced thioredoxin-interacting protein gene expression in pancreatic islets

Pradeep Bompada[a], David Atac[a], Cheng Luan[b], Robin Andersson[a], Judit Domènech Omella[a], Emilia Ottosson Laakso[a], Jason Wright[c], Leif Groop[a,d], Yang De Marinis[a,*]

[a] Diabetes and Endocrinology, Department of Clinical Sciences, Lund University, Malmö, SE-20502, Sweden
[b] Lund University Diabetes Centre, Department of Clinical Sciences, Lund University, Malmö, SE-20502, Sweden
[c] Broad Institute of Massachusetts Institute of Technology (MIT) and Harvard, Cambridge, MA, 02142, USA
[d] Finnish Institute for Molecular Medicine (FIMM), Helsinki University, Helsinki, FI-00014, Finland

ARTICLE INFO

Article history:
Received 29 April 2016
Received in revised form 20 October 2016
Accepted 24 October 2016
Available online 29 October 2016

Keywords:
Glucotoxicity
Beta cell
Histone acetylation
Histone acetyltransferase p300
Histone deacetylase
Thioredoxin-interacting protein

ABSTRACT

Thioredoxin-interacting protein (TXNIP) has been shown to be associated with glucose-induced deterioration of pancreatic beta cell function in diabetes. However, whether epigenetic mechanisms contribute to the regulation of *TXNIP* gene expression by glucose is not clear. Here we studied how glucose exerts its effect on *TXNIP* gene expression via modulation of histone acetylation marks. To achieve this, we applied clustered regularly interspaced short palindromic repeats/Cas9 (CRISPR/Cas9) to knock out histone acetyltransferase (HAT) p300 in a rat pancreatic beta cell line INS1 832/13. We also treated the cells and human islets with chemical inhibitors of HAT p300 and histone deacetylase (HDAC). In human islets, diabetes and high glucose resulted in elevated *TXNIP* and *EP300* expression, and glucose-induced *TXNIP* expression could be reversed by p300 inhibitor C646. In INS1 832/13 cells, *Ep300* knock-out by CRISPR/Cas9 elevated glucose-induced insulin secretion and greatly reduced glucose-stimulated *Txnip* expression and cell apoptosis. This effect could be ascribed to decrease in histone marks H3K9ac and H4ac at the promoter and first coding region of the *Txnip* gene. Histone marks H3K9ac and H4ac in the *Txnip* gene in the wild-type cells was inhibited by HDAC inhibitor at high glucose, which most likely was due to enhanced acetylation levels of p300 after HDAC inhibition; and thereby reduced p300 binding to the *Txnip* gene promoter region. Such inhibition was absent in the *Ep300* knock-out cells. Our study provides evidence that histone acetylation serves as a key regulator of glucose-induced increase in *TXNIP* gene expression and thereby glucotoxicity-induced apoptosis.

1. Introduction

In diabetes, elevated glucose levels over time induce beta cell dysfunction, as well as loss of beta cell mass via accelerated apoptosis rate (Butler et al., 2003; Maechler et al., 1999; Robertson et al., 1992). Such hyperglycemia-induced deterioration of pancreatic beta cell is referred to as glucotoxicity, which may involve changes in gene profiles and its underlying mechanisms remained to be elucidated (Robertson et al., 2003).

Previous studies have shown that thioredoxin-interacting protein (TXNIP), an endogenous inhibitor of the antioxidant protein thioredoxin (Chen et al., 2008; Oslowski et al., 2012; Parikh et al., 2007), is among the most highly upregulated genes in glucose-treated human islets and diabetic mouse islets (Minn et al., 2005). Glucose-induced *TXNIP* gene expression resulted in oxidative damage and beta cell death, suggesting an important role for TXNIP in linking glucotoxicity and beta cell apoptosis (Chen et al., 2008; Minn et al., 2005). A recent study showed that changes in DNA methylation of the *TXNIP* gene in peripheral blood are strongly associated with type 2 diabetes (T2D) incidence (Chambers et al., 2015). It has also been shown that glucose-induced *TXNIP* gene expression involves interaction of the carbohydrate response element binding protein (ChREBP) with histone acetyltransferase p300 at the promoter of the gene (Cha-Molstad et al., 2009a). These observations support the view that glucose could induce *TXNIP* gene expression via epigenetic mechanisms, e.g. modification of histone acetylation.

* Corresponding author at: Yang De Marinis, Inga Marie Nilssons gata 53 floor 3, Lund University Hospital (Malmö), SE-205 02 Malmö, Sweden.
E-mail address: Yang.de_marinis@med.lu.se (Y. De Marinis).

http://dx.doi.org/10.1016/j.biocel.2016.10.022
1357-2725/

Initiation of gene transcription involves relaxation of chromatin and unfolding of nucleosomes by various histone modifications including acetylation of the histones tails (Kouzarides, 2007; Narlikar et al., 2002). Histone acetylation is regulated by two groups of enzyme, HATs and histone deacetylases (HDACs). HATs add acetyl groups to the conserved lysine amino acids and this process can be reversed by removal of acetyl groups by HDACs. Gene transcription can be activated or repressed by lysine residue hyperacetylation or hypoacetylation regulated by both HAT and HDAC (Kuo and Allis, 1998; Yuan et al., 2013).

Although it is not clear if HAT gene expression and activity is affected by diabetes state in pancreatic islets, previous studies in other tissues have shown that HAT activity and histone acetylation is increased in kidneys of diabetic mice (Wang et al., 2015; Cai et al., 2016; De Marinis et al., 2016), as well as increased p300 gene expression in diabetic rat heart (Aziz et al., 2013). Inhibition of p300 by chemical inhibitor curcumin has been shown to prevent renal damage and dysfunction in streptozotocin (STZ)-induced diabetic mice (Wang et al., 2015). It could be reasonable to explore whether a similar mechanism also operates in pancreatic islets and, hence if p300 could be a potential therapeutic target to prevent beta cell damage in diabetes.

Here we examined HAT p300 (*EP300*) and *TXNIP* gene expression in diabetic human islets as well as rat insulinoma cell line INS1 832/13 exposed to high glucose. We have investigated whether inhibition of histone acetylation by either CRISPR/Cas9 silencing or a HAT p300 inhibitor could reverse glucose-increased *TXNIP* gene expression and rescue cells from glucose-induced apoptosis. Our study therefore shed light on a novel non-glucose lowering strategy for prevention of glucotoxicity in pancreatic islets by targeting at epigenetic mechanisms.

2. Materials and methods

2.1. Human Islets, cell culture and treatment

Human Islets from cadaver donors were provided by the Nordic Islet Transplantation Program. RNA-seq on islet samples was performed using Illumina's TruSeq RNA Sample Preparation Kit. All procedures were approved by the ethics committee at Lund University. Insulin secreting rat insulinoma cell line INS1 832/13 cells were cultured in complete RPMI 1640 medium (Invitrogen) containing 5 or 25 mM glucose. In the experiments testing the effect of p300 inhibitor, cells were treated with 25 μM C646 (Calbiochem, CA, USA) or 25 μM CI994 (Selleckchem, Houston, TX, USA) for 24 h in 5 or 25 mM glucose.

2.2. mRNA extraction and quantitative RT-PCR

Human islet and INS1 832/13 cell mRNA were extracted using RNeasy kit (QIAGEN) according to the manufacturer's instructions. mRNA was then reverse transcribed to cDNA using the first strand cDNA synthesis kit (Fermentas). mRNA expression was assessed by quantitative RT-PCR performed on a Prism 7900 Sequence Detection System by Taqman assay (Applied Biosystems). *Ep300* expression in human islets was normalized to two housekeeping genes *HPRT1* and *PPIB*. The assay numbers are: *HPRT1* Hs02800695_m1; *PPIB* Hs00168719_m1; *EP300* Hs00914223_m1; *TXNIP* Hs00197750. *Txnip* expression in rat pancreatic beta cell line INS1 832/13 was normalized to two housekeeping genes *Ppib* and *Gapdh*. The assay numbers are: *Gapdh* Rn01775763_g1; *Ppib* Rn03302274_m1; *Txnip* Rn01533885_g1.

2.3. Genome editing by CRISPR/Cas9

Ep300 −/− cells were generated applying CRISPR/Cas 9-mediated genome editing (Wu et al., 2014). INS1 832/13 cells were edited using nuclease Cas9 together with two guide RNA pairs that specifically target at exon 1 of *Ep300* (5′-AGATGAGAGTTTAGGCCGCT-3′ and 5′-GCGTCCGCCAGCGATGGCAC-3′). Guide sequence oligos were cloned into plasmid pX330-U6-Chimeric_BB-CBh-hSpCas9 (Addgene plasmid # 42230), a generous gift from Prof. Feng Zhang (Broad Institute of MIT and Harvard, Cambridge, MA, USA), and validated by Sanger sequencing. INS1 832/13 cells were then transfected with the constructed plasmids and single cell colonies were isolated by limiting dilution and expansion. Clones were then genotyped by Sanger sequencing in total 700 bp starting from 100 bp before the exon 1 of rat *Ep300* gene.

2.4. ChIP assay

Briefly, cells were cross-linked by formaldehyde (final concentration 1%) and sonicated by Bioruptor sonicator (Diagenode) for 30 cycles of 30-s with a 30-s interval (medium intensity) period between cycles. Genomic DNA fragment lengths of 200–1000 bp were achieved after sonication. Lysates were then centrifuged, and the supernatants (sonicated chromatin) were collected. 10% volume of each sample was removed as the input control. The sonicated chromatin was incubated overnight at 4 °C with 2.5 μg of antibody lysine 9-acetylated histone H3 (H3K9ac, ab4441, Abcam), H4ac (06-866, Millipore), p300 (sc-48343X, Santa Cruz Biotechnology) or a normal rabbit polyclonal IgG (12-370, Upstate/Millipore) as a negative control. Immune complexes were captured with 10 μl of 50% protein G beads, eluted by reverse cross-linking and protease K digestion. DNA fragments were purified using MinElute PCR Purification Kit (Qiagen) and quantified by SYBR Green PCR (Applied Biosystems) with primers designed for *Txnip* promoter region (forward primer AATGTTCCCCAACCTCACAG and reverse CTTCGTTCCATGCCCTATGT); and the first coding region of the gene (forward primer CGAGTCAAAGCCGTCAGGAT and reverse TTCATAGCGCAAGTAGTCCAAGGT). The DNA quantitation value of each sample was analyzed by the $2^{-D\Delta Ct}$ method and results were expressed as fold over control after normalizing with input samples. In all experiments, we verified that ChIP precipitation enrichment obtained was relative to IgG controls.

2.5. Western blotting

Cells were homogenized in ice-cold RIPA buffer containing complete protease inhibitor (Roche) by shaking on ice for 30 min. Supernatant was collected by centrifugation (10,000 × *g*, 10 min, 4 °C). Extracted total protein content was measured by Pierce BCA Protein Assay Kit (Thermo Scientific), and 8 μg of protein was electrophoresed by SDS- PAGE (BIO-RAD). The transferring and blocking were performed and the membrane was incubated overnight at 4 °C with anti-Acetyl-p300 antibody (Cell signalling, 1:1000) followed by incubation with anti-rabbit IgG (Cell Signaling, 1:2000) for 2 h at room temperature. Normalization was carried out by incubating membrane with anti-beta actin antibody (Sigma, 1:2000). Final signal was indicated by ChemiDoc MP System (BIO-RAD).

2.6. Insulin secretion assay

Insulin secretion was measured from cell culture medium by Mercodia High Range Rat Insulin ELISA kit (Mercodia AB), and nor-

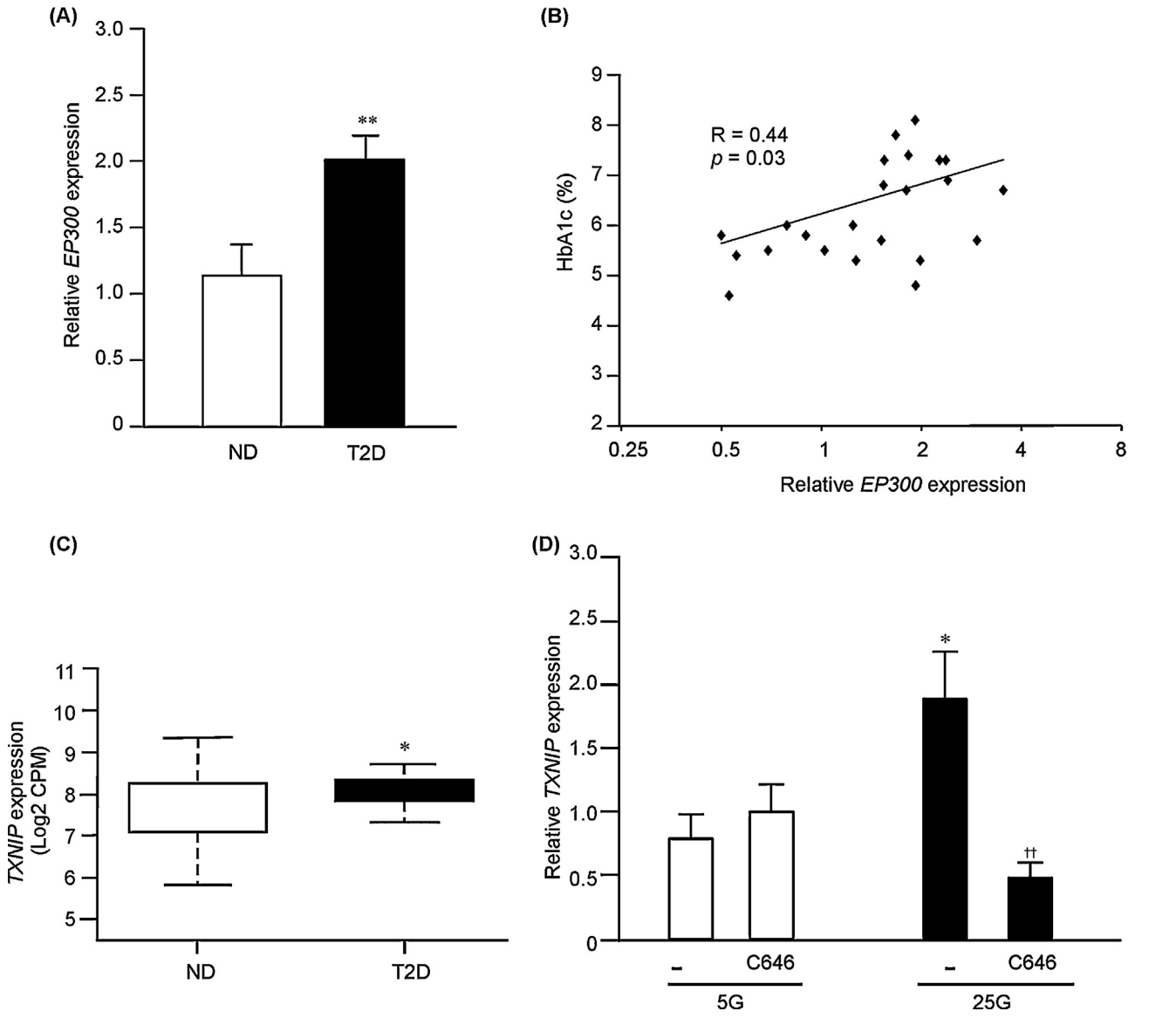

Fig. 1. Elevated *EP300* and *TXNIP* gene expression in human diabetic islets and inhibition of glucose-stimulated *TXNIP* expression by HAT p300 inhibitor. (A) *EP300* gene expression in human islets from non-diabetic (ND, white bar, n = 7) and type 2 diabetic donor (T2D, black bar, n = 11) was measured by TaqMan assay quantitative PCR and normalized to housekeeping genes *HPRT* and *PPIB*. $^{**}p < 0.01$ vs. ND. (B) Correlation between *EP300* gene expression in human islets and HbA_{1c} levels (between 4.6–8.1) in 23 donors. $p < 0.05$ was considered to be significant. (C) *TXNIP* gene expression was quantified by RNA sequencing in human islets from non-diabetic (ND, white box, n = 114) and diabetic (T2D, black box, n = 17) donors. $^{*}p < 0.05$ vs. ND. (D) Human islets from individual donors (n = 4–5) were treated in 5 (5G, white bars) or 25 mM glucose (25G, black bars), in the presence or absence of p300 inhibitor C646 (25 μM) for 24 h. *TXNIP* gene expression was measured by TaqMan assay quantitative PCR and normalized to housekeeping genes *HPRT* and *PPIB*. $^{*}p < 0.05$ vs. 5G control; and $^{††}p < 0.01$ vs. 25G control.

malized according to total protein content per well (measured by Pierce BCA Protein Assay Kit <Thermo Scientific>).

2.7. Cell growth measurement and apoptosis assay

Cells were trypsinized and collected after respective incubation conditions. Total cell number was then determined by automated cell counter (Orflo). Cell apoptosis was measured using Cell Death Detection ELISA kit (Roche).

2.8. Data analysis

Statistical comparisons were performed using 2-tailed Student's *t*-test if not stated otherwise. Data are expressed as the mean ± SEM. Correlations were analyzed by Pearson's correlation coefficient test. Differences with $p < 0.05$ were considered significant.

3. Results

3.1. Elevation of EP300 and TXNIP gene expression in human diabetic islets and reduction of glucose-stimulated TXNIP gene expression by inhibition of p300

To study whether HAT p300 gene (*EP300*) expression is affected by the diabetic state, we examined *EP300* expression in human islets from non-diabetic and T2D donors by quantitative PCR. *EP300* gene expression was almost doubled in T2D islets (Fig. 1A) and correlated strongly with HbA_{1c} levels (Fig. 1B), suggesting that increased *EP300* gene expression could be a consequence of hyperglycemia.

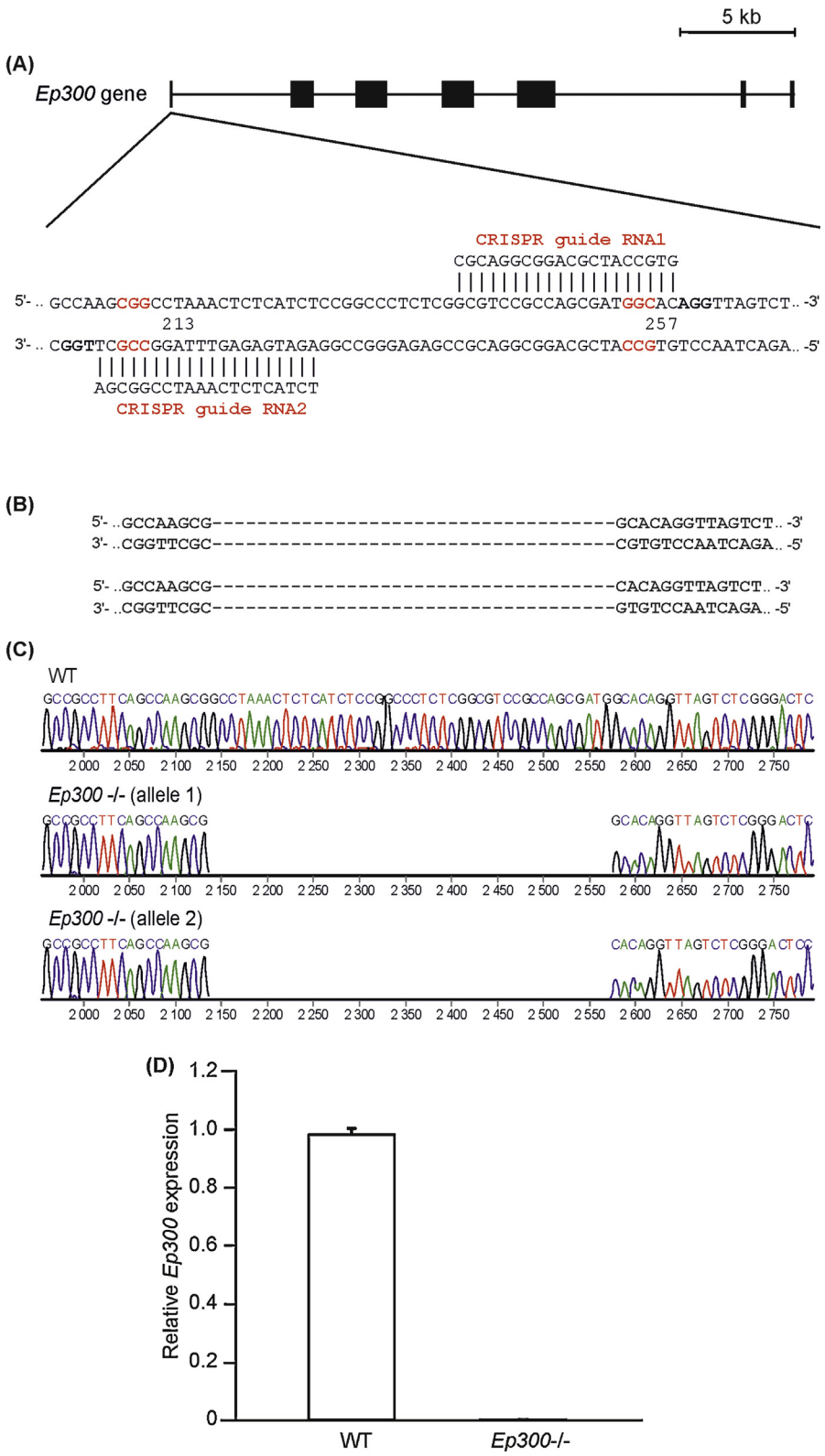

Fig. 2. CRISPR/Cas9 silencing of *Ep300* in INS1 832/13 cells. (A) Two CRISPR guide RNAs were designed to respectively bind 3 bps before the end of *Ep300* exon 1 (CRISPR guide RNA 1) and 41 bps from the beginning of exon 1 (CRISPR guide RNA 2). PAM sequences are highlighted in black bold letters and CRISPR cutting sites are highlighted in red bold letters. (B) Illustration of *Ep300* exon 1 deletion with 44 bps deletion on one allele and 45 bps deletion on the other allele. (C) Chromatogram confirmation of the deletion by Sanger sequencing. (D) *Ep300* expression in wild-type and *Ep300* knock-out cells was quantified by qPCR and normalized to housekeeping genes *Gapdh* and *Ppib* expression. The values represent the mean ± SEM of three independent experiments. (For interpretation of the references to colour in this figure legend, the reader is referred to the web version of this article.)

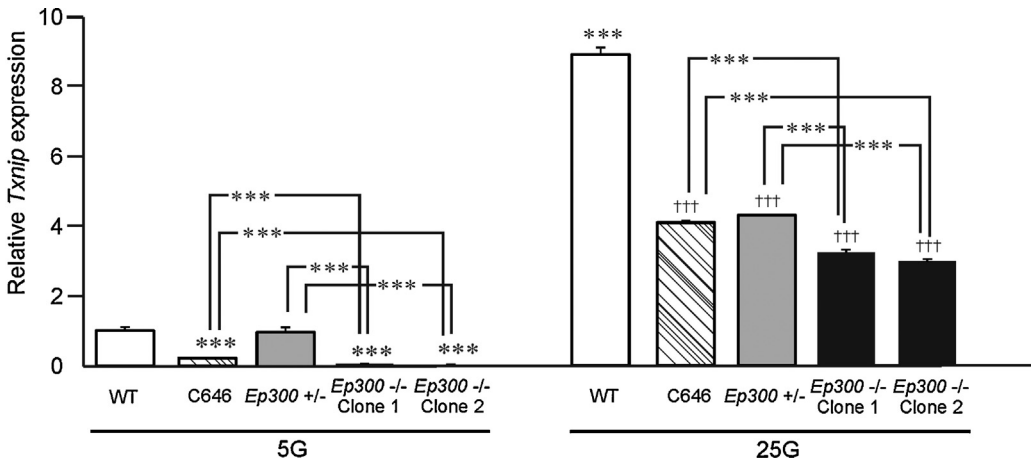

Fig. 3. Reduced *Txnip* gene expression in *Ep300* knock-out cells. Glucose-stimulated *Txnip* gene expression was significantly decreased in INS1 832/13 cells with *Ep300* CRISPR/Cas9 knock-out. Wild-type (open bars), wild-type treated with HAT p300 inhibitor C646 (25 μM, hatched bars), *Ep300* heterozygous knock-out (grey bars) and *Ep300* homozygous knock-out (black bars) cells were incubated in 5 (5G) or 25 mM glucose (25G) for 24 h. mRNA was isolated and *Txnip* gene expression was quantified by qPCR and normalized to housekeeping gene *Gapdh* and *Ppib* expression. The values represent the mean ± SEM of six independent experiments. ***$p < 0.001$ vs. 5G control or as indicated; †††$p < 0.001$ vs. 25G control.

In the transcriptome from 131 human donors, we detected significantly increased *TXNIP* gene expression in T2D islets compared to non-diabetic islets (Fig. 1C). Previous studies have shown that glucose stimulates recruitment of p300 to the promoter region of the *TXNIP* gene in human islet (Cha-Molstad et al., 2009a). To investigate if glucose-stimulated *TXNIP* gene expression can be reduced by inhibition of p300, we incubated human islets for 24 h in 5 or 25 mM glucose in the presence or absence of p300 inhibitor C646. We observed significant reduction in high glucose-induced *TXNIP* gene expression by C646 (Fig. 1D), which suggests that glucose-induced increase in *TXNIP* expression can be prevented by inhibition of p300.

3.2. Reduced glucose-stimulated increase in Txnip gene expression in a rat pancreatic beta cell line after ep300 knockout

To further delineate the role of p300 in histone acetylation of the *TXNIP* gene and its consequences on gene transcription, we created a target deletion of *Ep300* exon 1 by CRISPR/Cas9 in a rat pancreatic beta cell line INS1 832/13. We designed two CRISPR guide RNAs (gRNAs) that respectively bind 41 bps after the beginning of exon 1, and 3 bps before the end of exon 1 (Fig. 2A). As Cas9 nuclease introduces DNA breaks 3–4 bps (Fig. 2A, sequences highlighted in red) before a PAM sequence (Fig. 2A, sequences highlighted in black), we obtained a clone with deletion of exon 1 in the *Ep300* gene with 45 bps deletion in one allele and 44 bps deletion in the other allele (Fig. 2B), which was confirmed by Sanger sequencing (Fig. 2C). Quantitative PCR (qPCR) using *Ep300* TaqMan assays showed complete absence of *Ep300* expression (Fig. 2D). Wild-type, homozygous and heterozygous clones used in the following experiments were identified and confirmed by Sanger sequencing.

We then treated wild-type, *Ep300* +/− (heterozygous deletion) and *Ep300* −/− (homozygous deletion) INS1 832/13 cells in 5 or 25 mM glucose for 24 h. Wild-type cells were also treated with p300 inhibitor C646 at both glucose concentrations to compare the effect of the inhibitor on *Txnip* expression to that of CRISPR/Cas9 knock-out. To rule out the possibility of off-targets by CRISPR/Cas9, we tested the effect of two *Ep300* −/− clones with exon 1 deletion introduced by CRISPR/Cas9 (as shown in Fig. 3, *Ep300* −/− Clone 1 and 2). Cells were collected after treatment and relative *Txnip* mRNA levels were measured by qPCR (Fig. 3). Basal *Txnip* expression at 5 mM glucose was significantly reduced by C646, as well as in *Ep300* −/− clones. High glucose (25 mM) increased *Txnip* expression, which was greatly reduced by C646. Heterozygous *Ep300* +/− had similar *Txnip* expression reduction compared to C646-treated wild-type. In homozygous *Ep300* −/− clones, *Txnip* expression was significantly lower than in C646-treated wild-type or *Ep300* +/− cells.

3.3. Effect of Ep300 knock-out and HDAC inhibition on histone acetylation at the promoter and the first coding region of the Txnip gene and gene expression

To study in detail the effect of *Ep300* knock-out on histone acetylation in the *Txnip* gene, we performed chromatin immunoprecipitation (ChIP) on wild-type and *Ep300* −/− cells using antibodies binding to histone 3 lysine 9 acetylation (H3K9ac) and histone 4 acetylation (H4ac) which are frequently acetylated sites in active gene transcription. Since histone acetylation is regulated by both HATs and histone deacetylases (HDACs) in a counteracting and balanced manner, to study if the effect of *Ep300* knock-out on histone acetylation can be reversed by HDAC inhibition, we also treated the cells with a class I HDAC inhibitor CI994. Wild-type and *Ep300* −/− cells were incubated 24 h in 5 and 25 mM glucose, in the presence and absence of CI994. ChIP-quantitative PCR (ChIP-qPCR) for H3K9ac and H4ac enrichment was performed on sheared and precipitated DNA from the cells using primers flanking the promoter region and the first coding region of the *Txnip* gene (Fig. 4 A–F). We observed that at 5 mM glucose, CI994 increased H3K9ac and H4ac at promoter in both wild-type and *Ep300* −/− cells to similar extend (Fig. 4B and C). In the first coding region, CI994 increased H3K9ac and H4ac in the wild-type, but only H3K9ac in the *Ep300* −/− cells (Fig. 4E and F). High glucose significantly increased H3K9ac and H4ac in the *Txnip* gene in the wild-type cells, and this increase was greatly reduced in the *Ep300* −/− cells (Fig. 4B–F). In both wild-type and *Ep300* −/− cells, high glucose increased H4ac at the promoter (Fig. 4C), H3K9ac and H4ac in the first coding region (Fig. 4E and F). While high glucose-increased H3K9ac at the promoter was only observed in the wild-type but not in *Ep300* −/− cells. Surprisingly, in wild-type, CI994 decreased H4ac at the promoter (Fig. 4C), H3K9ac and H4ac at the first coding region (Fig. 4E and F); but had no effect on H3K9ac at the promoter (Fig. 4B). In the *Ep300* −/− cells, CI994 increased H3K9ac at the promoter (Fig. 4B), and had no effect on any other acetylation events examined (Fig. 4C–F).

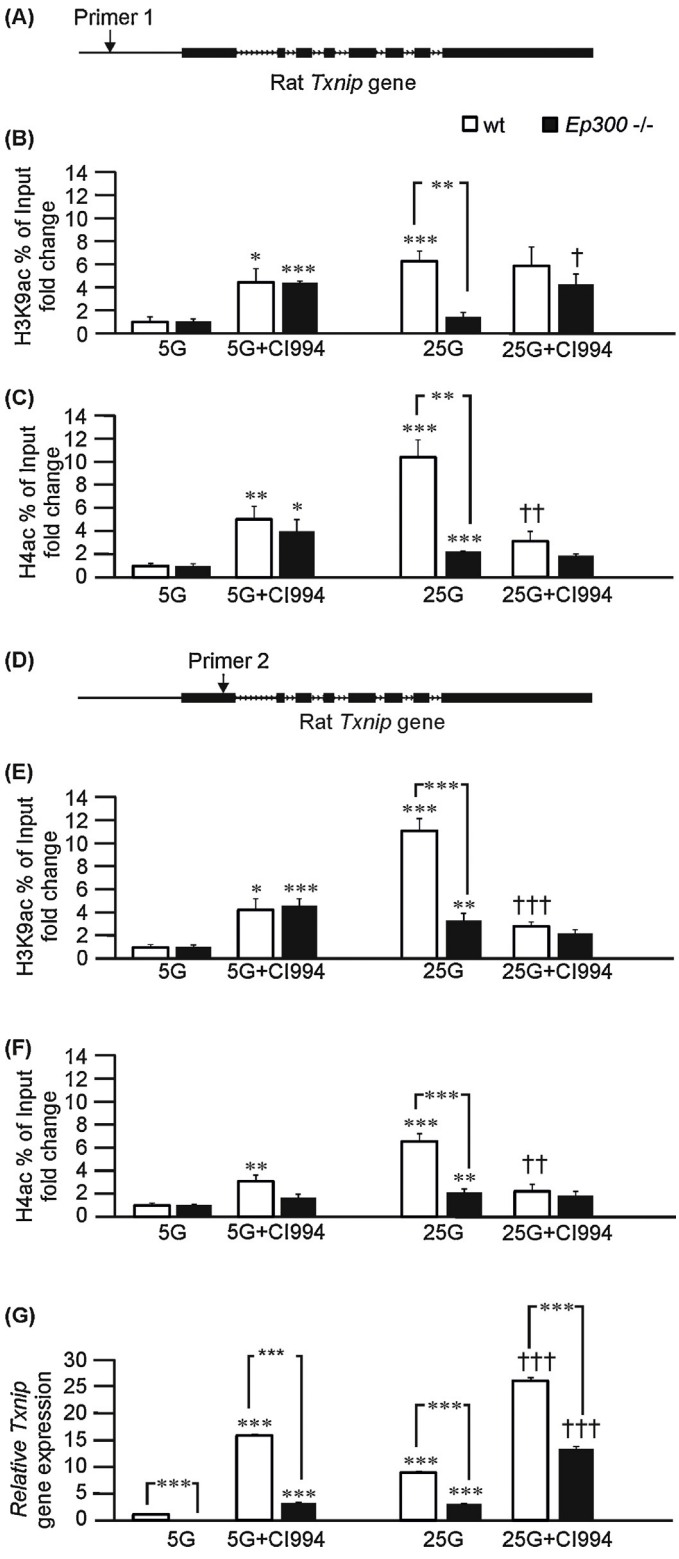

Fig. 4. Effect of *Ep300* knock-out on histone acetylation at the promoter and the first coding region of the *Txnip* gene and reduction in *Txnip* gene expression. (A) Schematic of the ChIP-qPCR primer location is indicated by large arrow. Primer 1 locates at −600 bp from the +1 transcription start site of *Txnip* gene. Exons are presented as filled rectangles. (B, C) Wild-type cells (white bars) and *Ep300* −/− cells (black bars) were incubated in 5 (5G) or 25 mM glucose (25G), in the presence or absence of HDAC inhibitor CI994 (25 μM) for 24 h. Cells were then fixed and sonicated. DNA was precipitated using antibodies binding to H3K9ac (B) or H4ac (C). Quantitative PCR was run using primers flanking the promoter region as indicated in (A), and results are presented as fold change over 5G. The values represent the mean ± SEM of four to five independent experiments. $^{*}p < 0.05$, $^{**}p < 0.01$, $^{***}p < 0.001$ vs. respective 5G (wild-type or knock out) or as indicated; $^{\dagger}p < 0.05$, $^{\dagger\dagger}p < 0.01$ vs. 25G. (D) Schematic of the ChIP-PCR primer location is indicated by large arrow. Primer 2 locates within exon 1 of *Txnip* gene. Exons are presented as filled rectangles. (E, F) ChIP-PCR was run on the same ChIP DNA from (B) and (C) using primers flanking the first coding region as indicated in (D). Enrichment of H3K9ac (E) and H4ac (F) were presented as fold changes over 5G. $^{*}p < 0.05$, $^{**}p < 0.01$, $^{***}p < 0.001$ vs. respective 5G (wild-type or knock out) or as indicated; $^{\dagger\dagger}p < 0.01$, $^{\dagger\dagger\dagger}p < 0.001$ vs. 25G. The values represent the mean ± SEM of four to five independent experiments. (G) Wild-type (white bars) and *Ep300* −/− (black bars) cells were treated 24 h with 5 (5G) or 25 mM glucose (25G), with or without HDAC inhibitor C646 (25 μM). mRNA was isolated and *Txnip* expression was quantified by qPCR and normalized to housekeeping gene *Gapdh* and *Ppib* expression. The values represent the mean ± SEM of six independent experiments. $^{***}p < 0.001$ vs. 5G or as indicated; $^{\dagger\dagger\dagger}p < 0.001$ vs. 25G.

To study if the observed changes in acetylation had any impact on *Txnip* gene expression, we performed qPCR on cells collected from the same experiments as in ChIP. CI994, 25 mM glucose, or in combination, significantly increased *Txnip* gene expression in both wild-type and *Ep300* −/−, but to a much reduced extend in the *Ep300* −/− cells (Fig. 4G).

3.4. An HDAC inhibitor decreased p300 binding to the Txnip promoter by increasing p300 autoacetylation

Previous studies have shown that there are multiple regions of p300 susceptible to autoacetylation by p300 (Stiehl et al., 2007), and p300 undergoes a dynamic cycle of autoacetylation by itself and deacetylation by HDACs (Black et al., 2008). Conformational changes caused by autoacetylation will change binding affinity of p300 to gene promoter. We therefore speculate that the reduction of H3K9ac and H4K9 at high glucose in the presence of HDAC inhibitor CI994 (Fig. 4C, E and F) is due to increased acetylated p300 and thereby decreased binding to the *Txnip* promoter. To test this hypothesis, we first performed western blotting using antibody binding to acetylated p300 (ac-p300) on INS1 832/13 cells treated with 5 and 25 mM glucose, in the presence and absence of CI994. Ac-p300 was significantly lower in high glucose compared to low glucose, and CI994 increase ac-p300 at both glucose concentrations (Fig. 5A). Next, we studied p300 binding at the *Txnip* promoter and first coding region by ChIP. High glucose had a tendency ($p = 0.08$) to increase p300 binding at the *Txnip* promoter, which was significantly reduced by CI994, while p300 binding at the first coding region of *Txnip* was relatively low and not affected by either glucose concentration or CI994 (Fig. 5B).

3.5. Reduced Txnip gene expression by Ep300 knock-out increased insulin secretion and prevented glucotoxicity by reducing apoptosis and promoting cell growth

TXNIP has been shown to act as a negative regulator of cell growth and metabolism (Elgort et al., 2010; Parikh et al., 2007; Patwari et al., 2009) and induces beta cell apoptosis (Chen et al., 2010). To study if reduced *Txnip* gene expression in *Ep300* −/− cells promotes insulin secretion, we treated wild-type and *Ep300* −/− cells in 5 and 25 mM glucose for 24 h. Insulin secretion was significantly increased in the knock-out cells at both glucose concentrations (Fig. 6) compared to the wild-type. To investigate if *Ep300* knock out protects beta cells from glucotoxicity-induced apoptosis, cell apoptosis was measured in wild-type and *Ep300* −/− cells treated in 5 and 25 mM glucose for 48 and 72 h. We observed that high glucose-induced cell death was greatly reduced; and cell growth was increased in *Ep300* −/− cells compared to wild-type already after 48 h and persisted for 72 h (Fig. 7A). We performed similar cell apoptosis assay in INS1 832/13 cells treated with 5 or 25 mM glucose, with or without C646 and CI994. Both inhibitors increased cell death with less fold increase at high glucose, during

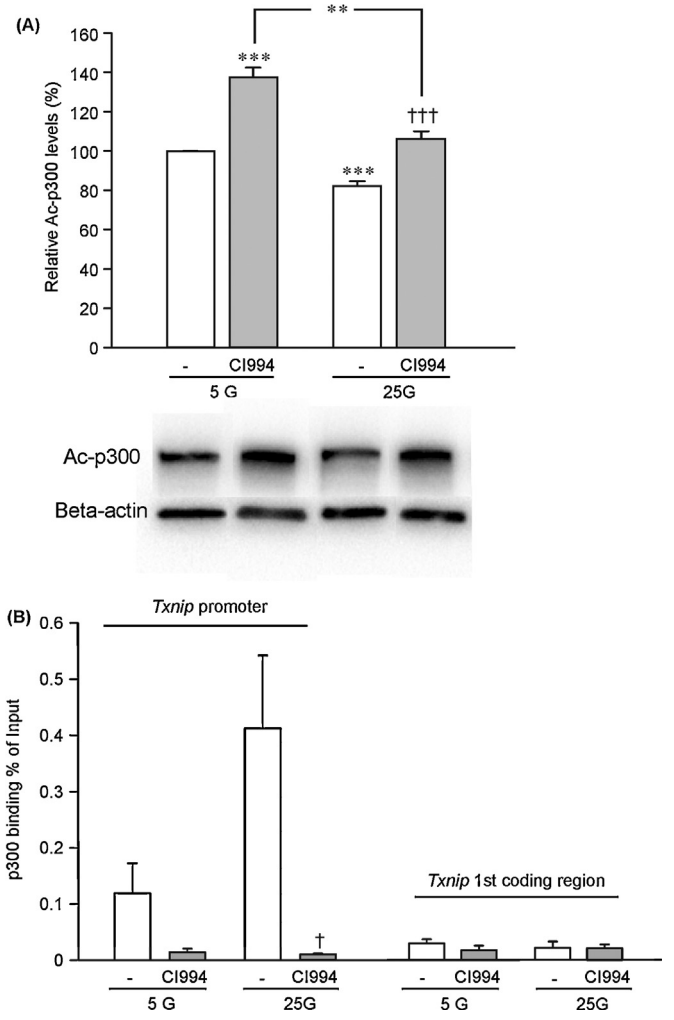

Fig. 5. Increased acetylated p300 and decreased p300 binding at *Txnip* promoter by CI994. (A) INS1 832/13 cells were incubated 24 h in 5 (5G) or 25 mM glucose (25G) with (n = 5, grey bars) or without CI994 (n = 5, white bars). Cells were then collected for western blotting using antibody binding to acetylated-p300 (A); or ChIP using antibodies binding to p300 (B). ChIP PCR was run using primers flanking the promoter and 1 st coding region, and results are presented as p300 binding % of input. The values represent the mean ± SEM. $^{***}p < 0.001$ vs. 5G or as indicated; $^{\dagger}p < 0.05$, $^{\dagger\dagger\dagger}p < 0.001$ vs. 25G.

which condition p300 activity increases and is more susceptible to inhibition. Therefore the lower fold change suggests a protective effect of the inhibitors at high glucose (Fig. 8).

4. Discussion

Increased *TXNIP* gene expression in pancreatic islets is considered a hallmark of glucotoxicity and a mediator of the negative effects of glucose on beta-cells. The novel finding of this work was the demonstration of involvement of HAT p300 and HDACs on *TXNIP* gene expression via histone acetylation in pancreatic beta cells. We investigated in detail by applying pharmacological inhibitors of p300 and HDACs, as well as silencing of *Ep300* gene using CRISPR/Cas9).

Previous studies have shown that high glucose increases acetylation at H4ac in the promoter region of the *TXNIP* gene (Cha-Molstad et al., 2009a). However, it has not been demonstrated if glucose-induced *TXNIP* gene expression can be reversed by targeting at HAT. Here we provide evidence that glucose-stimulated *Txnip* gene expression is dependent on p300-facilited histone acetylation. Beside pharmacological inhibitor, we also applied p300 silencing by

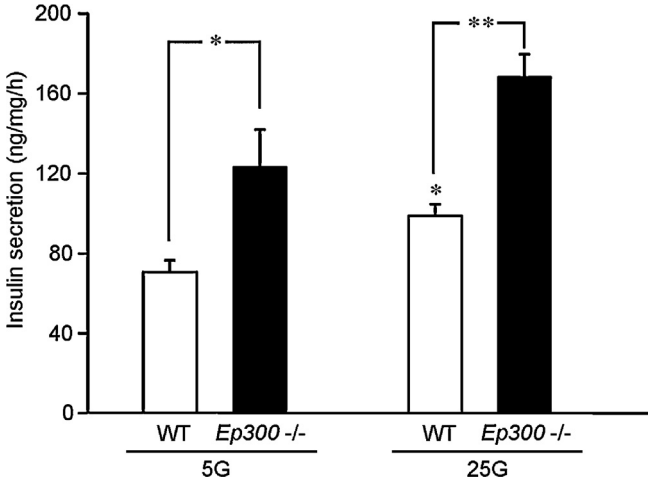

Fig. 6. Increased insulin secretion in Ep300 knock-out cells. Wild-type cells (n = 12, white bars) and Ep300 −/− cells (n = 12, black bars) were incubated in 5 (5G) or 25 mM glucose (25G) for 24 h. Insulin secretion was then determined by Mercodia High Range Rat Insulin ELISA kit (Mercodia AB). The values represent the mean ± SEM. $^{*}p < 0.05$, $^{**}p < 0.01$ vs. wild-type 5G or as indicated.

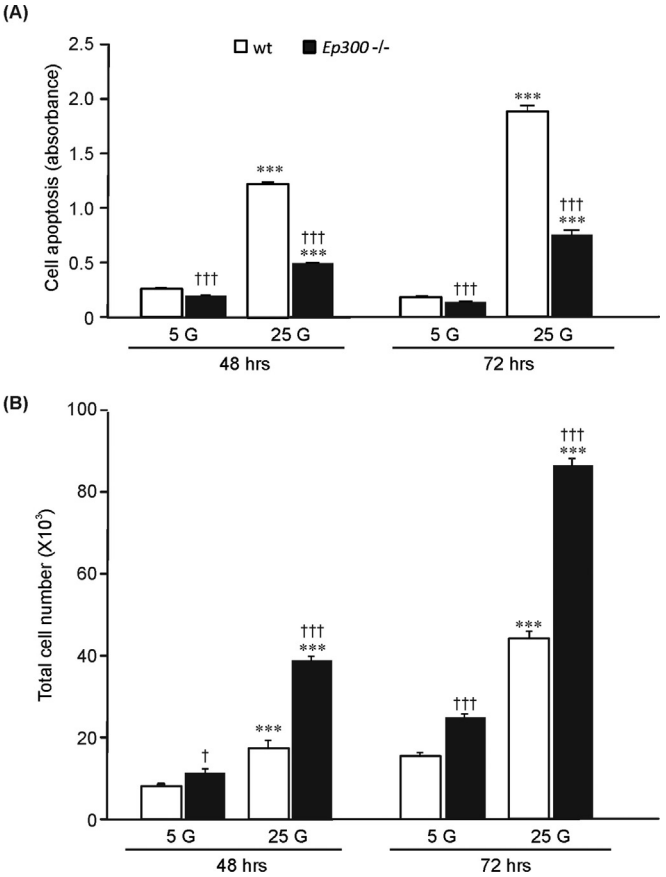

Fig. 7. Reduced cell apoptosis and promotion of cell growth in *Ep300* knock-out cells. Wild-type cells (n = 6, white bars) and *Ep300* −/− cells (n = 6, black bars) were incubated in 5 (5G) or 25 mM glucose (25G) for 48 or 72 h as indicated. (A) Cell apoptosis was then determined by Cell Death Detection ELISA kit (Roche). The values represent the mean ± SEM. $^{***}p < 0.001$ vs. 5G (wild-type or knock out, respectively); $^{\dagger\dagger\dagger}p < 0.001$ vs. wild-type of the same condition. (B) Cells number was counted by automated cell counter (Orflo). The values represent the mean ± SEM. $^{***}p < 0.001$ vs. 5G (wild-type or knock out, respectively); $^{\dagger\dagger\dagger}p < 0.001$ vs. respective wild-type.

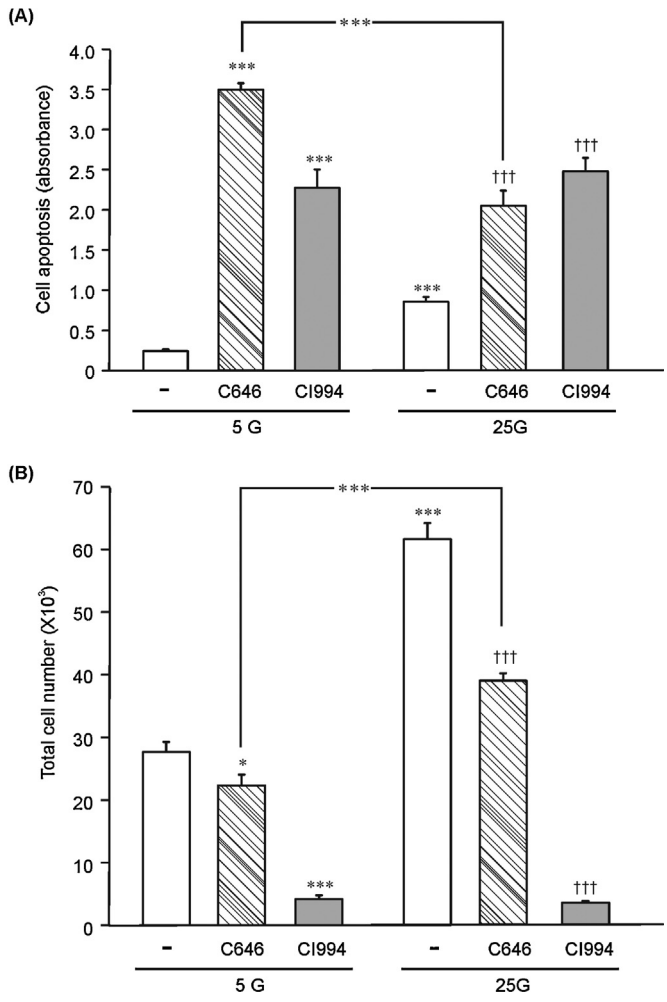

Fig. 8. Increased cell apoptosis and reduction of cell growth in wild type cells exposed to HAT inhibitor C646 and HDAC inhibitor CI994. Wild-type cells were incubated in 5 (5G) or 25 mM glucose (25G) with (shaded bar) and without (open bars) C646 (n = 6) and CI994 (n = 6) for 72 h. (A) Cell apoptosis was measured by Cell Death Detection ELISA kit (Roche). The values represent the mean ± SEM. ***$p < 0.001$ vs. 5G or as indicated; †††$p < 0.001$ vs. 25G. (B) Cell number was counted by automated cell counter (Orflo). The values represent the mean ± SEM. *$p < 0.05$, *** $p < 0.001$ vs. 5G or as indicated; †††$p < 0.001$ vs. 25G.

CRISPR/Cas9. Although studies have shown that CRISPR/Cas9 has very limited off-target effects comparing to Zinc finger nucleases (ZFNs) and transcription activator-like effector nucleases (TALENS) (Duan et al., 2014), one of the major concerns of genome editing by CRISPR/Cas9 is unexpected off-target events which may lead to undesired mutations and phenotypes. Methods such as whole genome sequencing has been suggested for validation of off-targets, however, it has limitations in sequence depth and possibility to miss out heterozygous mutations (Kim et al., 2016). Therefore, in our study, we confirmed the absence of off-target by demonstrating equal effects of two homozygous clones on reduction of down-stream *Txnip* gene expression, as well as an intermediate effect on heterozygous clone (Fig. 3).

Histone marks H3K9ac and H4ac of the *Txnip* gene were increased at 5 mM glucose by the HDAC inhibitor CI994 (Fig. 4B–F). This observation is in line with previous studies where HDAC inhibitor TSA increased H4 acetylation and thereby *Txnip* (Cha-Molstad et al., 2009b) and insulin (Mosley and Ozcan, 2003) gene expression at low glucose concentrations. There was no significant difference between the effect of CI994 in wild-type and *Ep300* −/− cells at low glucose, indicating that the stimulatory effect of CI994 on H3K9ac and H4ac at 5 mM glucose is independent of p300. High glucose (25 mM) increased histone acetylation in both wild-type and *Ep300* −/−, the latter had markedly reduced acetylation levels (Fig. 4b–f), indicating high glucose-increased histone acetylation in *Txnip* gene is largely dependent on p300. This was further supported by the finding that in *Ep300* −/− cells, glucose-increased histone acetylation was not affected by addition of CI994. A surprising observation was that in the wild-type, CI994 significantly decreased high glucose-increased histone acetylation (Fig. 4B–F). It has been shown that p300 is susceptible to autoacetylation by itself (Stiehl et al., 2007), and deacetylation by HDACs (Black et al., 2008). Conformational changes caused by autoacetylation and deacetylation will therefore change binding affinity of p300 to various complexes. Silencing of HDAC SIRT2 has been shown to increase p300 autoacetylation and thereby decrease p300 recruitment to the Luciferase promoter and decrease downstream gene expression (Black et al., 2008). Here in our study, reduction of glucose-increased histone acetylation by CI994 was absent in *Ep300* −/−, suggesting that the inhibitory effect of HDAC inhibitor CI994 on histone acetylation at high glucose is p300 dependent. Furthermore, we provided evidence that p300 acetylation is decreased by high glucose and increased by HDAC inhibitor (Fig. 5A). The latter resulted in decreased p300 binding to the *Txnip* promoter (Fig. 5B); and as a consequence, reduced histone acetylation (Figs. 4 and 9). Although *Txnip* gene expression was also increased by CI994 at high glucose in the wild-type (Fig. 4G), the fold change (2.9-fold) was less than that seen in *Ep300* −/− (4.2-fold).

In this study, we investigated changes in histone acetylation marks H3K9ac and H4ac. However, there are many more histone marks that are susceptible to acetylation, such as H2AK5, H2BK8, H3K14, H3K18, H3K23 etc. At 5 mM glucose, *Ep300* −/− decreased; and HDAC inhibitor CI994 increased *Txnip* gene expression, but had no significant effect on H3K9ac and H4ac. This may be a consequence of modification of other histone acetylation marks. Previous studies have shown that acetyl-CoA concentrations alter the histone acetylation pattern by altering p300 specificity (Henry et al., 2015). Free energy analysis has shown that H3K9 has the least p300 affinity among histone acetylation marks at low acetyl-CoA levels, while having the highest affinity at high acetyl-CoA concentrations generated by metabolism of glucose. Therefore we speculate that the changes in H3K9ac and H4ac in association with gene expression at low/high glucose may be due to changes in p300 specificity and affinity to the modification sites.

Taken together, glucose-induced *Txnip* gene expression is greatly reduced by p300 silencing, and *Ep300* −/− cells are protected from high glucose-induced cell death and have elevated insulin secretion. Since expression of both *Ep300* and *Txnip* is elevated in human diabetic islets, prevention of glucose-induced histone acetylation could present a new therapeutic strategy to protect pancreatic beta cells from glucotoxicity.

Duality of interest

The authors declare that there is no duality of interest associated with this manuscript.

Author contributions

P.B. performed in vitro experiments and analysis. D.A. performed in vitro experiments and analysis. C.L. performed in vitro experiments and analysis. R.A. performed in vitro experiments and analysis. J.D. performed in vitro experiments and analysis. E.O.L. performed in vitro experiments and analysis. J.W. performed in vitro experiments. L.G. designed and supervised all parts of the study and drafted the report. Y.D.M. designed the study, performed in vitro experiments and analysis, supervised all parts of the study

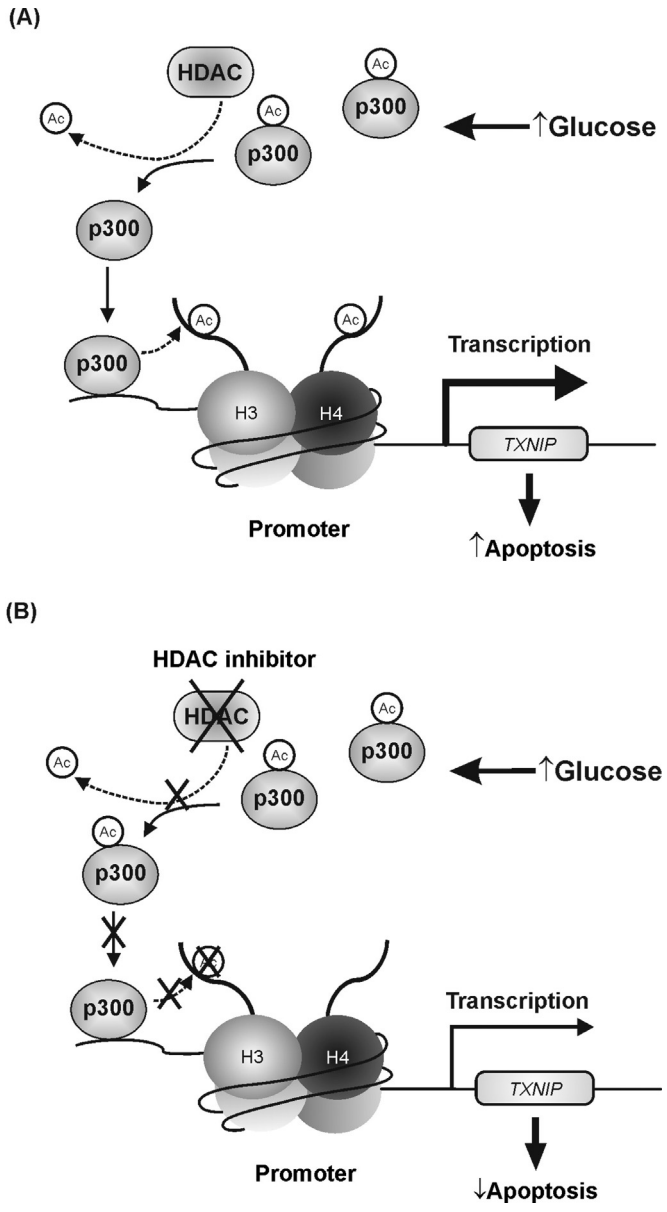

Fig. 9. Schematic model for glucose-stimulated *TXNIP* gene expression mediated by histone acetylation. (A) At high glucose, the acetyl groups from acetylated p300 are dynamically removed by HDAC and the non-acetylated p300 binds to the *TXNIP* gene promoter. Histone acetylation at H3K9ac and H4ac facilitated by p300 will result in increased *TXNIP* gene expression which leads to beta cell apoptosis. (B) At the presence of an HDAC inhibitor, p300 remains in the acetylated state, which results in reduced p300 occupancy at the *TXNIP* gene promoter and decreased H3K9ac and H4ac.

and drafted the report. All researchers took part in the revision of the report and approved the final version.

Acknowledgements

The work was supported by grants to Leif Groop from the Swedish Research Council: a project grant (Nr 2010-3490) and a Centre of Excellence Grant to the Lund University Diabetes Centre (Nr 2008-6589), and by the European Union's Seventh Framework. This work was also supported by grants from the Hjelt Foundation.

References

Aziz, M.T., El Ibrashy, I.N., Mikhailidis, D.P., Rezq, A.M., Wassef, M.A., Fouad, H.H., Ahmed, H.H., Sabry, D.A., Shawky, H.M., Hussein, R.E., 2013. Signaling mechanisms of a water soluble curcumin derivative in experimental type 1 diabetes with cardiomyopathy. Diabetol. Metab. Syndr. 5 (1), 13.

Black, J.C., Mosley, A., Kitada, T., Washburn, M., Carey, M., 2008. The SIRT2 deacetylase regulates autoacetylation of p300. Mol. Cell 32 (3), 449–455.

Butler, A.E., Janson, J., Bonner-Weir, S., Ritzel, R., Rizza, R.A., Butler, P.C., 2003. Beta-cell deficit and increased beta-cell apoptosis in humans with type 2 diabetes. Diabetes 52 (1), 102–110.

Cai, M., Bompada, P., Atac, D., Laakso, M., Groop, L., De Marinis, Y., 2016. Epigenetic regulation of glucose-stimulated osteopontin (OPN) expression in diabetic kidney. Biochem. Biophys. Res. Commun. 469 (1), 108–113.

Cha-Molstad, H., Saxena, G., Chen, J., Shalev, A., 2009a. Glucose-stimulated expression of Txnip is mediated by carbohydrate response element-binding protein, p300, and histone H4 acetylation in pancreatic beta cells. J. Biol. Chem. 284 (25), 16898–16905.

Cha-Molstad, H., Saxena, G., Chen, J.Q., Shalev, A., 2009b. Glucose-stimulated expression of Txnip is mediated by carbohydrate response element-binding protein, p300, and histone H4 acetylation in pancreatic beta cells. J. Biol. Chem. 284 (25), 16898–16905.

Chambers, J.C., Loh, M., Lehne, B., Drong, A., Kriebel, J., Motta, V., Wahl, S., Elliott, H.R., Rota, F., Scott, W.R., Zhang, W., Tan, S.T., Campanella, G., Chadeau-Hyam, M., Yengo, L., Richmond, R.C., Adamowicz-Brice, M., Afzal, U., Bozaoglu, K., Mok, Z.Y., Ng, H.K., Pattou, F., Prokisch, H., Rozario, M.A., Tarantini, L., Abbott, J., Ala-Korpela, M., Albetti, B., Ammerpohl, O., Bertazzi, P.A., Blancher, C., Caiazzo, R., Danesh, J., Gaunt, T.R., de Lusignan, S., Gieger, C., Illig, T., Jha, S., Jones, S., Jowett, J., Kangas, A.J., Kasturiratne, A., Kato, N., Kotea, N., Kowlessur, S., Pitkaniemi, J., Punjabi, P., Saleheen, D., Schafmayer, C., Soininen, P., Tai, E.S., Thorand, B., Tuomilehto, J., Wickremasinghe, A.R., Kyrtopoulos, S.A., Aitman, T.J., Herder, C., Hampe, J., Cauchi, S., Relton, C.L., Froguel, P., Soong, R., Vineis, P., Jarvelin, M.R., Scott, J., Grallert, H., Bollati, V., Elliott, P., McCarthy, M.I., Kooner, J.S., 2015. Epigenome-wide association of DNA methylation markers in peripheral blood from Indian Asians and Europeans with incident type 2 diabetes: a nested case-control study. Lancet Diabetes Endocrinol. 3 (7), 526–534.

Chen, J., Saxena, G., Mungrue, I.N., Lusis, A.J., Shalev, A., 2008. Thioredoxin-interacting protein: a critical link between glucose toxicity and beta-cell apoptosis. Diabetes 57 (4), 938–944.

Chen, J., Fontes, G., Saxena, G., Poitout, V., Shalev, A., 2010. Lack of TXNIP protects against mitochondria-mediated apoptosis but not against fatty acid-induced ER stress-mediated beta-cell death. Diabetes 59 (2), 440–447.

De Marinis, Y., Cai, M., Bompada, P., Atac, D., Kotova, O., Johansson, M.E., Garcia-Vaz, E., Gomez, M.F., Laakso, M., Groop, L., 2016. Epigenetic regulation of the thioredoxin-interacting protein (TXNIP) gene by hyperglycemia in kidney. Kidney Int. 89 (2), 342–353.

Duan, J.Z., Lu, G.Q., Xie, Z., Lou, M.L., Luo, J., Guo, L., Zhang, Y., 2014. Genome-wide identification of CRISPR/Cas9 off-targets in human genome. Cell Res. 24 (8), 1009–1012.

Elgort, M.G., O'Shea, J.M., Jiang, Y., Ayer, D.E., 2010. Transcriptional and translational downregulation of thioredoxin interacting protein is required for metabolic reprogramming during G(1). Genes Cancer 1 (9), 893–907.

Henry, R.A., Kuo, Y.M., Bhattacharjee, V., Yen, T.J., Andrews, A.J., 2015. Changing the selectivity of p300 by acetyl-CoA modulation of histone acetylation. ACS Chem. Biol. 10 (1), 146–156.

Kim, D., Kim, S., Kim, S., Park, J., Kim, J.S., 2016. Genome-wide target specificities of CRISPR-Cas9 nucleases revealed by multiplex Digenome-seq. Genome Res. 26 (3), 406–415.

Kouzarides, T., 2007. Chromatin modifications and their function. Cell 128 (4), 693–705.

Kuo, M.H., Allis, C.D., 1998. Roles of histone acetyltransferases and deacetylases in gene regulation. BioEssays 20 (8), 615–626.

Maechler, P., Jornot, L., Wollheim, C.B., 1999. Hydrogen peroxide alters mitochondrial activation and insulin secretion in pancreatic beta cells. J. Biol. Chem. 274 (39), 27905–27913.

Minn, A.H., Hafele, C., Shalev, A., 2005. Thioredoxin-interacting protein is stimulated by glucose through a carbohydrate response element and induces beta-cell apoptosis. Endocrinology 146 (5), 2397–2405.

Mosley, A.L., Ozcan, S., 2003. Glucose regulates insulin gene transcription by hyperacetylation of histone H4. J. Biol. Chem. 278 (22), 19660–19666.

Narlikar, G.J., Fan, H.Y., Kingston, R.E., 2002. Cooperation between complexes that regulate chromatin structure and transcription. Cell 108 (4), 475–487.

Oslowski, C.M., Hara, T., O'Sullivan-Murphy, B., Kanekura, K., Lu, S., Hara, M., Ishigaki, S., Zhu, L.J., Hayashi, E., Hui, S.T., Greiner, D., Kaufman, R.J., Bortell, R., Urano, F., 2012. Thioredoxin-interacting protein mediates ER stress-induced beta cell death through initiation of the inflammasome. Cell Metab. 16 (2), 265–273.

Parikh, H., Carlsson, E., Chutkow, W.A., Johansson, L.E., Storgaard, H., Poulsen, P., Saxena, R., Ladd, C., Schulze, P.C., Mazzini, M.J., Jensen, C.B., Krook, A., Bjornholm, M., Tornqvist, H., Zierath, J.R., Ridderstrale, M., Altshuler, D., Lee, R.T., Vaag, A., Groop, L.C., Mootha, V.K., 2007. TXNIP regulates peripheral glucose metabolism in humans. PLoS Med. 4 (5), e158.

Patwari, P., Chutkow, W.A., Cummings, K., Verstraeten, V.L., Lammerding, J., Schreiter, E.R., Lee, R.T., 2009. Thioredoxin-independent regulation of metabolism by the alpha-arrestin proteins. J. Biol. Chem. 284 (37), 24996–25003.

Robertson, R.P., Zhang, H.J., Pyzdrowski, K.L., Walseth, T.F., 1992. Preservation of insulin mRNA levels and insulin secretion in HIT cells by avoidance of chronic exposure to high glucose concentrations. J. Clin. Invest. 90 (2), 320–325.

Robertson, R.P., Harmon, J., Tran, P.O., Tanaka, Y., Takahashi, H., 2003. Glucose toxicity in beta-cells: type 2 diabetes, good radicals gone bad, and the glutathione connection. Diabetes 52 (3), 581–587.

Stiehl, D.P., Fath, D.M., Liang, D.M., Jiang, Y.B., Sang, N.L., 2007. Histone deacetylase inhibitors synergize p300 autoacetylation that regulates its transactivation activity and complex formation. Cancer Res. 67 (5), 2256–2264.

Wang, Y., Wang, Y., Luo, M., Wu, H., Kong, L., Xin, Y., Cui, W., Zhao, Y., Wang, J., Liang, G., Miao, L., Cai, L., 2015. Novel curcumin analog C66 prevents diabetic nephropathy via JNK pathway with the involvement of p300/CBP-mediated histone acetylation. Biochim. Biophys. Acta 1852 (1), 34–46.

Wu, X., Scott, D.A., Kriz, A.J., Chiu, A.C., Hsu, P.D., Dadon, D.B., Cheng, A.W., Trevino, A.E., Konermann, S., Chen, S., Jaenisch, R., Zhang, F., Sharp, P.A., 2014. Genome-wide binding of the CRISPR endonuclease Cas9 in mammalian cells. Nat. Biotechnol. 32 (7), 670–676.

Yuan, H., Reddy, M.A., Sun, G., Lanting, L., Wang, M., Kato, M., Natarajan, R., 2013. Involvement of p300/CBP and epigenetic histone acetylation in TGF-beta1-mediated gene transcription in mesangial cells. Am. J. Physiol. Renal Physiol. 304 (5), F601–613.